ICIC Express Letters
Volume **12**, Number **12**, December **2018**
 ISSN 1881-803X
pp. **1183–1193**

IMPROVING THE RELIABILITY OF *F*-STATISTIC METHOD BY USING LINEAR SUPPORT VECTOR MACHINE FOR STRUCTURAL HEALTH MONITORING

Fergyanto Efendy Gunawan

Industrial Engineering Department, BINUS Graduate Program – Master of Industrial Engineering
Bina Nusantara University
Jl. K. H. Syahdan No. 9, Kemanggisan, Palmerah, Jakarta 11480, Indonesia
fgunawan@binus.edu

Received May 2018; accepted August 2018

Abstract. *We address the issue of reliability of F-statistic method for predicting the structural integrity on the basis of the vibration data. The method is traditional but to the best of the author's knowledge, its weaknesses and reliability have not been explored. As this work demonstrates, the use of the method often leads to false-positive predictions, where intact structures are predicted to be damaged, and false-negative predictions, where damaged structures are predicted to be intact. We claim the use of the statistic in conjunction with a linear classification model should improve the prediction accuracy. To demonstrate the claim, 17494 examples of data are established from a numerical simulation of a seven-degree-of-freedom model, which is widely studied in the field of structural health monitoring. Then, the data are divided into two groups with the ratio of 70:30 for model development and testing. A linear classification model is established by minimizing a combination of a hinge loss function and a regularization loss function. An optimal regularization parameter is also determined. The present approach is able to increase the classification accuracy by about 10%.*
Keywords: Structural health monitoring, F-statistic, Support vector machine

1. **Introduction.** On Nov. 26, 2011, at 16:20 local time, 10-year-old Kutai Kertanegara bridge in Samarinda, Indonesia, suddenly collapsed (Figure 1). As the results, 24 persons died, 39 injured, and 12 were missing. It also took down dozens of cars and motor vehicles [1]. On July 3, 2014, in Belo Horizonte, Brazil, a fly-over broke down instantly, killed two persons, and injured 22 [2]. We often heard engineering structures collapse catastrophically due to overloads, abrasion, or erosion [3], but most often, corrosion, metal fatigue, and overload were the culprit according to a study involving 6000 accidents [4] (Table 1).

Most structures require regular monitoring either manually or automatically by using a system (SHM). Manual inspection is susceptible to human errors and unreliable [3]. Small-size cracks, the most common cause of aircraft failure [5], often go undetected. SHM system has the potential to provide reliable, accurate, and low-cost monitoring system. SHM has been widely applied to rotating machineries [6, 7], aircraft structures [8, 9], bridges [10, 11], and railways [12, 13, 14].

For SHM system to work, data acquired from structure, from which damage sensitive features are derived, and predictive models where the features are linked to structural integrity should be provided. So far, scientists have utilized neural networks [16, 17, 18, 19] or support vector machine [20, 21] to establish the predictive models, and have used vibration data to provide damage sensitive features such as natural frequencies and mode shapes [24, 25, 26, 27, 28, 29], modal curvatures [30, 31, 32], modal strain energies [33], spectral moments [9, 34], and time series [35].

DOI: 10.24507/icicel.12.12.1183

FIGURE 1. The collapsed Kutai Kertanegara bridge [1]

TABLE 1. The frequency of various failure mechanisms [4]

	Percentage of failures	
	Engineering components	Aircraft components
Corrosion	29	16
Fatigue	25	55
Brittle fracture	16	–
Overload	11	14
High temperature corrosion	7	2
SCC/corrosion fatigue/HE	6	7
Creep	3	–
Wear/abrasion/erosion	3	6

In the vibration-based SHM, F-statistic is known to be damage sensitive [40], easy to compute, and had been experimentally verified [41]. However, its reliability, the rate of false classifications where a healthy structure is detected as damaged and vice versa, has not been addressed. This research investigates the level of the reliability that can be achieved by the use of F-statistic in an idealized condition and a method to improve the reliability.

This article is organized as the following. Section 2 presents the research procedure including the data collection method, feature extraction method, and the linear support vector machine (SVM). Section 3 presents the distributions of the F-statistic and the classification reliability with and without SVM. Section 4 presents the most important findings of the work.

2. **Research Methods.**

2.1. **Data collection method.** Data are produced by a numerical analysis of a seven-degree-of-freedom system (Figure 2). The system consists of seven lumped masses, 1 kg each, connected by eight similar linear elastic springs, each has 1 N/m stiffness. A dynamic force having a random magnitude is applied to the center mass. The force magnitude

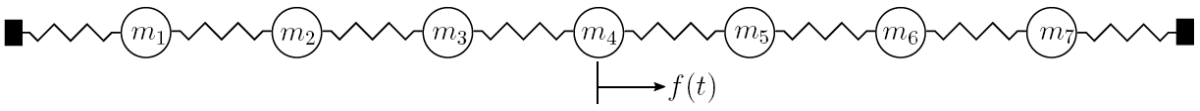

FIGURE 2. The model of seven-degree-of-freedom system

is drawn from a normal probabilistic distribution with a mean of zero and a standard deviation of 0.09. Initially, the random force data have frequency contents up to 25 Hz. Then, the data are filtered with a Butterworth filter with a cutoff frequency of 20 Hz and an order of 12.

The structural damage is assumed to occur on the spring connecting m_3 and m_4. It is also assumed to affect the spring and to degrade its stiffness only. Four levels of the degradation are studied, namely, 1%, 5%, 10%, and 20%. This decision is made to understand how the damage level affects the accuracy of the classification. We hypothesize that the classification accuracy is low when the damage level is low, the relation between the classification accuracy and the damage level is not linear, and when the damage level is higher than certain threshold, the classification accuracy is independent to the damage level.

The analysis results are the displacement of the seven masses. The data are sampled at a constant rate of 0.1 s and for a duration of 360 s. For each structural condition, the analysis is repeated for 500 times by varying the distribution of the dynamic force. The settings of the applied dynamic force and the sampling rate of the structural responses are determined by considering the structure natural frequencies: 0.62, 1.22, 1.77, 2.25, 2.65, 2.94, and 3.12 in Hz. The frequencies ω are determined by solving the eigenvalue problem of $(\mathbf{K}-\omega^2\mathbf{M})\mathbf{\Phi}=\mathbf{0}$, where $\mathbf{K}$ is the stiffness matrix, $\mathbf{M}$ is the mass matrix, and $\mathbf{\Phi}$ is the eigenvector.

2.2. **Power density spectrum by Barlett's method.** In this research, F-statistic is used as the damage-sensitive feature. Its computation requires the power spectrum density (PSD) data, which are computed by the following procedure by using Barlett's method [43].

We consider an analog, time-varying, and finite-length signal $x_a(t)$. In SHM, the signal may represent the historical data of the displacement at an observation point. The signal is assumed to be measured at a constant sampling rate of t_s such that $x_i = x_a(i \cdot t_s)$ where $i = 0, 1, 2, \ldots, (N-1)$. We transform the discrete time-domain signal x_i into the frequency domain by applying the discrete Fourier transform with the formula: $X(f_k) = \sum_{i=0}^{N-1} x_i \cdot \exp(-ji2\pi f t_s)$ where $f \in [0, f_s/2]$ and $f_s = 1/t_s$, which is called the sampling frequency, and f_k are discrete frequencies of $f_i = i \cdot f_s/N$. To shorten the expression, we use the symbol X_i to denote $X(f_i)$. We partition the signal into M-equal-length sub signals as illustrated by Figure 3. Barlett's method computes a signal PSD by averaging PSDs of the sub signals. The resulted PSD is more reliable and less sensitive to the signal noises. However, the method is only applicable for long signals. The Barlett's formula for computing PSD is:

$$S_i(f) = \frac{1}{LM} \sum_{m=0}^{M-1} \left| X_i^{(m)} \right|^2 . \tag{1}$$

The signal length N and the number of sub signals M is related by $N = LM$, where L is the length of the sub signal.

2.3. ***F*-statistic for SHM.** The method is simple and practical, depending only on the data of structural responses, which can be collected on a few measurement points. It turns the damage monitoring problem into a directionless hypothesis test that can be solved in three steps.

The first is the statement of the null and alternative hypotheses, which for this case, are:

$$\mathrm{H}_0 : S_h(\omega) = S_u(\omega) \quad \text{and} \quad \mathrm{H}_\mathrm{a} : S_h(\omega) \neq S_u(\omega). \tag{2}$$

The symbol $S(\omega)$ denotes PSD. The subscript h denotes the healthy condition and u means the unknown-to-be-sought condition. The healthy condition is the reference condition, from which the other structural conditions is measured. It should be determined

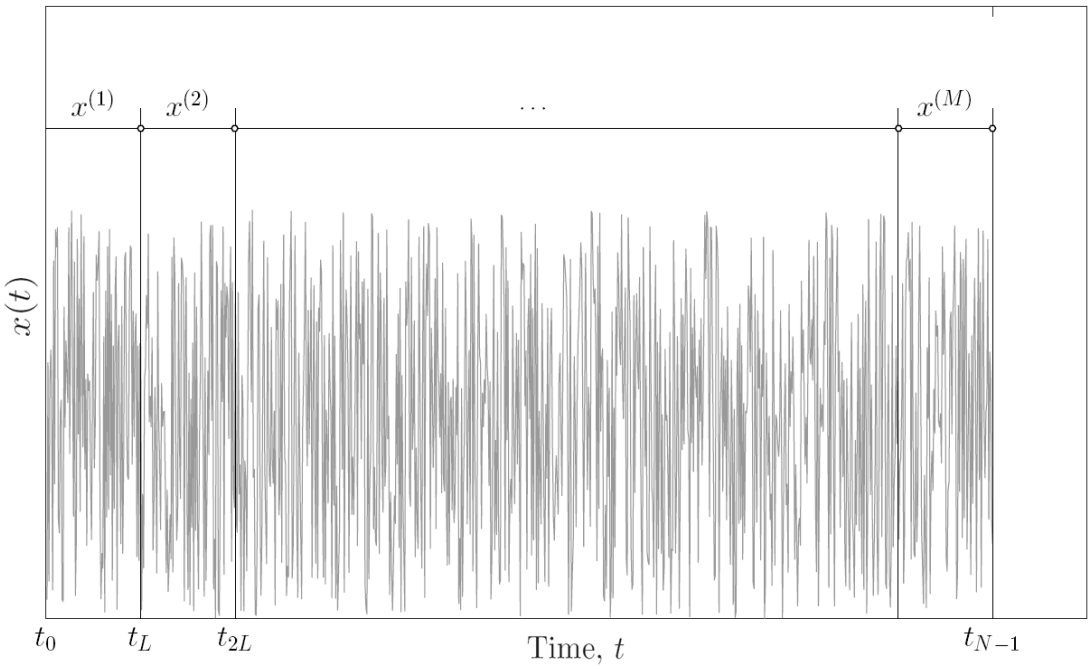

FIGURE 3. The partition of the signal $x(t)$ into M-equal-length sub signals

previously. The structure is assumed healthy if the null hypothesis H_0 prevails. It is considered healthy if its PSD is very much similar to the PSD of healthy condition. The degree of the similarity is measured statistically. The structure is assumed to contain damage if the alternative hypothesis H_a prevails, that is the PSDs have changed significantly. The structure associated with $S_u(\omega)$ is considered damaged if $S_u(\omega)$ deviates significantly from $S_h(\omega)$.

The second step is to compute the relevant F-statistic. This statistic is simply a comparison of two PSDs: $S_h(\omega)$ and $S_u(\omega)$. The statistic has the value of one when the two PSDs are exactly identical. When the structure contains damages, some values of the F-statistic may deviate from one becoming very big or very small. The level of change in PSD determines the magnitude of the F-statistic. The statistic is computed by: $F = \left[\hat{S}_h(\omega)/S_h(\omega)\right] \Big/ \left[\hat{S}_u(\omega)/S_u(\omega)\right]$. The hat denotes the estimated PSD. This expression can be made simpler. Under the condition of (2), it can be simplified to

$$F = \hat{S}_h(\omega)/\hat{S}_u(\omega). \tag{3}$$

The third is to establish the upper and lower limits of the statistic from which the change of PSD can be categorized as significant or not. The lower limit is $F_{(1-\alpha/2,2K,2K)}$ and the upper limit is $F_{(\alpha/2,2K,2K)}$. The symbol α denotes the statistical significance, which represents the probability of rejecting the null hypothesis given the structure condition is healthy. The symbol K denotes the degree of freedom, which represents the number of windows in the Barlett's method (see Subsection 2.2).

An expression similar to Equation (3), as discussed by [44], is extremely sensitive to perturbation, producing highly fluctuating statistic, often exceeding the lower and upper limits on a healthy structural condition. The F-statistic is unreliable and must be computed with a great care.

2.4. **Linear support vector machine.** For SHM, the F-statistic was utilized with a simple classification method. The structure was assumed damaged if the value of the F-statistic was greater than $F_{(\alpha/2,2K,2K)}$ or smaller than $F_{(1-\alpha/2,2K,2K)}$ [40, 41]. In contrast, the current study uses a more robust classification method, which allows us to use multiple values of the F-statistic.

In the present study, we only use the support vector machine (SVM) for linearly separable data. The SVM is a numerical method to compute a hyperplane for separating a two-class dataset. It can easily be extended to multiple-class problems. The SVM establishes the hyperplane, governed by $(\mathbf{w}, b)$, by using the support vectors, which are the data points that are closest to the hyperplane. The following SVM formulation is derived from [45, 46]; readers are advised to the two sources for detail exposition.

We consider the point sets $\mathbf{x}_i \in \Re^d$, as the support vectors, with the categories $y_i \in [-1, +1]$. The variable d is a positive integer. The hyperplane that separates $y_i = -1$ from those of $y_i = +1$ should satisfy

$$< \mathbf{w}, \mathbf{x} > +b = 0, \tag{4}$$

where $\mathbf{w} \in \Re^d$, $< \mathbf{w}, \mathbf{x} >$ denotes the inner dot product of $\mathbf{w}$ and $\mathbf{x}$, and b is a scalar constant. The hyperplane is obtained by solving the following cost function:

$$\min_{\mathbf{w},b} \frac{1}{2} \lambda < \mathbf{w}, \mathbf{w} > + \sum_i \left[1 - y_i \left(< \mathbf{w}, \mathbf{x}_i > +b\right)\right], \tag{5}$$

where $\lambda \geq 0$ is the fudge factor and is used to avoid over fitting. The first part of the loss function is referred as the regularization loss function and the second part is as the hinge loss function.

2.5. **Performance indicator and evaluation method.** We adopt five performance measures from [47] to evaluate the classification performance. They are: true positive rate (TPR), true negative rate (TNR), false positive rate (FPR), false negative rate (FNR), and accuracy. They are computed by the following formulas: $\mathrm{TPR} = \mathrm{TP}/(\mathrm{TP} + \mathrm{FN})$, $\mathrm{TNR} = \mathrm{TN}/(\mathrm{TN} + \mathrm{FP})$, $\mathrm{FPR} = \mathrm{FP}/(\mathrm{FP} + \mathrm{TN})$, $\mathrm{FNR} = \mathrm{FN}/(\mathrm{FN} + \mathrm{TP})$, $\mathrm{Accuracy} = (\mathrm{TP} + \mathrm{TN})/(\mathrm{TP} + \mathrm{TN} + \mathrm{FP} + \mathrm{FN})$ where TP is true positive, TN is true negative, FP is false positive, and FN is false negative. TPR is also called recall.

3. **Results.** The dataset used in the current study consists of 17494 cases with five structural conditions: healthy and damaged at the levels of 1%, 5%, 10%, and 20%. From each case, a few largest and smallest F-statistic values are extracted from the vibration data and are utilized as features to determine the structural conditions. The distribution of the F-statistic is depicted in Figure 4 for the largest and smallest values. We note that the y-axis of the figures are presented in the log scale because the F-statistic values may span a few order of magnitude.

Generally speaking, the largest F-statistic values tend to increase exponentially with the damage level. Meanwhile, the smallest F-statistic values tend to decrease exponentially with the damage level. Those figures also suggest that the F-statistic values on the

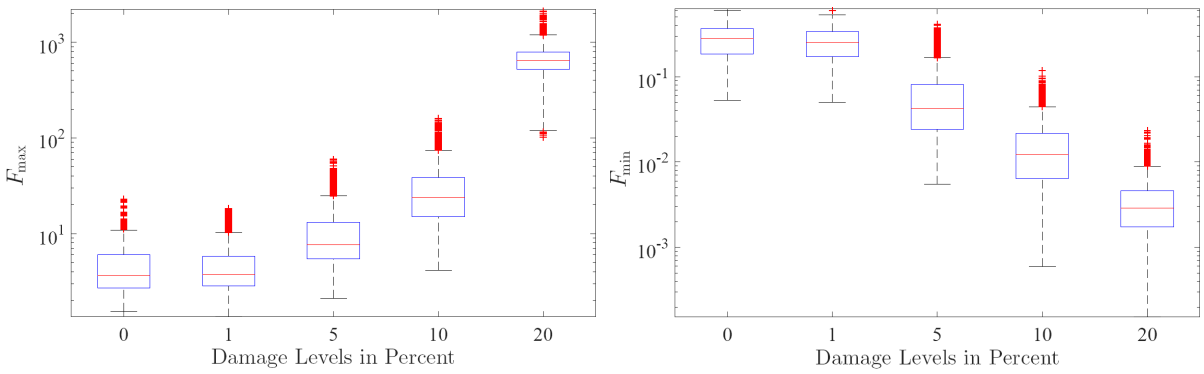

FIGURE 4. The distributions of the largest and smallest F-statistic values for the structure in the healthy and damaged conditions. The damage level of zero denotes the healthy condition.

healthy condition are distributed across almost similar range with those of the 1% damaged condition. Thus, differentiating the healthy condition from the damage condition on the basis of F-statistic is difficult when the damage level is small. The overlap between the distributions of the healthy condition and that of damage conditions is smaller with increasing the damage level, suggesting that identifying the damage condition is easier when the damage level is high. For those structures designed with the damage tolerance principles, the question lies on whether or not the identifiable damage level is within the allowable limit.

3.1. **The reliability of the existing method.** Firstly, let us discuss the level of the accuracy of the existing simple method for the current set of data. From a total of 17494 cases, the existing method is able to correctly predict 12707 cases, an accuracy level of 72.6%, or the error rate of 37.4%. A more detailed description of the performance of the simple method is in Table 2. TPR and TNR denote the rates of true predictions for both healthy and damaged conditions. It does show not only the results of using one value of the F-statistic, either the largest of the smallest, but also the results of using a few F-statistic values. The results are also separated according to the damage level. For the healthy condition, the simple classifier is able to provide the correct prediction by the rate of 73.3% up to 87.9% depending on the number of used features. The incorrect prediction rate is in 12.1-26.8 percents. When it contains small damage, the simple classifier is not able to satisfactorily differentiate the structure from a healthy one. The data show when the structure contains 1% damage, the correct prediction is only about 27.7% and the incorrect prediction is 72.3%. For the damage level of 5% or higher, the simple method is able to provide classification by 94.7% or more.

Table 2. The accuracy of the simple classification method

Datasets	#F-stats	TPR	TNR	FPR	FNR	Accuracy
Healthy	1	–	0.7323	0.2677	–	–
	2	–	0.7667	0.2333	–	–
	3	–	0.8786	0.1214	–	–
1% Damage	1	0.2774	–	–	0.7226	0.2774
	2	0.2203	–	–	0.7797	0.2203
	3	0.0709	–	–	0.9291	0.0709
5% Damage	1	0.9466	–	–	0.0534	0.9466
	2	0.8474	–	–	0.1526	0.8474
	3	0.6263	–	–	0.3737	0.6263
10% Damage	1	1.0000	–	–	0.0000	1.0000
	2	1.0000	–	–	0.0000	1.0000
	3	0.9989	–	–	0.0011	0.9989
20% Damage	1	1.0000	–	–	0.0000	1.0000
	2	1.0000	–	–	0.0000	1.0000
	3	1.0000	–	–	0.0000	1.0000
H-5%	1	0.9466	0.7323	0.2677	0.0534	0.6814
	2	0.8474	0.7667	0.2333	0.1526	0.6373
	3	0.6263	0.8786	0.1214	0.3737	0.5459

3.2. **Distribution of the estimated F-statistic.** A better picture regarding the probability characteristics of the estimated F-statistic and how the distribution is affected by the damage level is provided in Figure 5. The distribution deviates from the theoretical distribution significantly around the peak of the distributions at $F = 1$. Outside the region, the two distributions are rather identical. The distribution width increases with

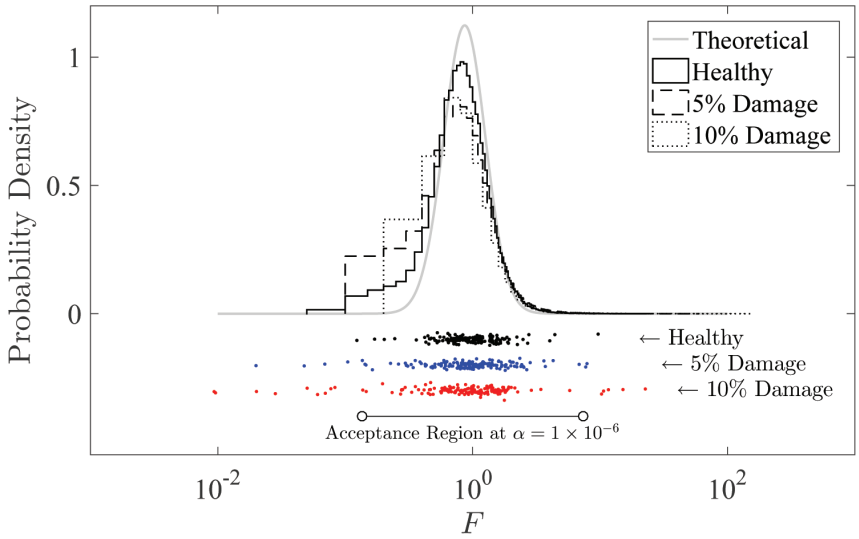

FIGURE 5. A comparison of the estimated F-statistic for the healthy and damaged structural conditions and the theoretical probability distribution

increasing the damage level. This fact suggests that a statistical parameter representing the distribution of data may be a better indicator of damage and its size.

3.3. **Optimization of the SVM model parameters.** The dataset containing 17494 cases is used to train and test the SVM model (4). The dataset is divided into two subsets with 70:30 ratio.

During the training phase, the SVM model coefficients of $\mathbf{w}$ and b are computed by minimizing Equation (5). To obtain the reliable model coefficients, the training process is performed carefully and a number of convergence characteristics are closely monitored during the iteration. The attention is given particularly to the changes of the cost function and its components during the iteration. In addition, the changes of the model coefficients and of the model predictive accuracy are also continuously observed.

At the learning rate of 1×10^{-4} and the fudge factor $\lambda = 50$, the computation converges quickly to the optimal solution (Figure 6(a)). Both the hinge and regularization loss functions decrease quickly for the first 50 iterations. Afterwards, the two functions tend to be unchanged with iterations. The regularization loss function flattens after 50 iterations. The hinge loss function still decreases but at a very low rate.

The convergence of $\mathbf{w}$ and b is depicted in Figure 6(b). The vector $\mathbf{w}$ converges monotonically to the best solution. When the computation is terminated at iteration 100, the change of the vector has become very small. The bias factor b initially decreases until the iteration 48, from which the bias factor slowly increases. The bias factor b converges much faster than the vector $\mathbf{w}$.

The change of the model prediction accuracy during the training phase is shown in Figure 6(c). The accuracy converges much faster than any previously discussed indicators. After the first iteration, the accuracy has reached the level of 77.8%. This occurs due to the use of the linear model and the use of large data for each training batch. The accuracy does not converge to a single value but changing with the batch data. For example, the accuracy increases for the first three batches of data, drops and then subsequently increases for the fourth, fifth, sixth, and seventh batches of data. The distribution of the accuracy is provided in a boxplot located on the upper-right corner of the figure. The statistics of the accuracy are: min. = 77.4%, $Q_1 = 79.8\%$, $Q_2 = 82.0\%$, $Q_3 = 83.0\%$, and max. = 85.3%. Finally, we conclude that the linear model is satisfactory numerically.

3.4. **The optimum fudge factor.** In the cost function of Equation (5), the penalty factor, the fudge factor λ, is used to avoid the model over fitting the training data. If

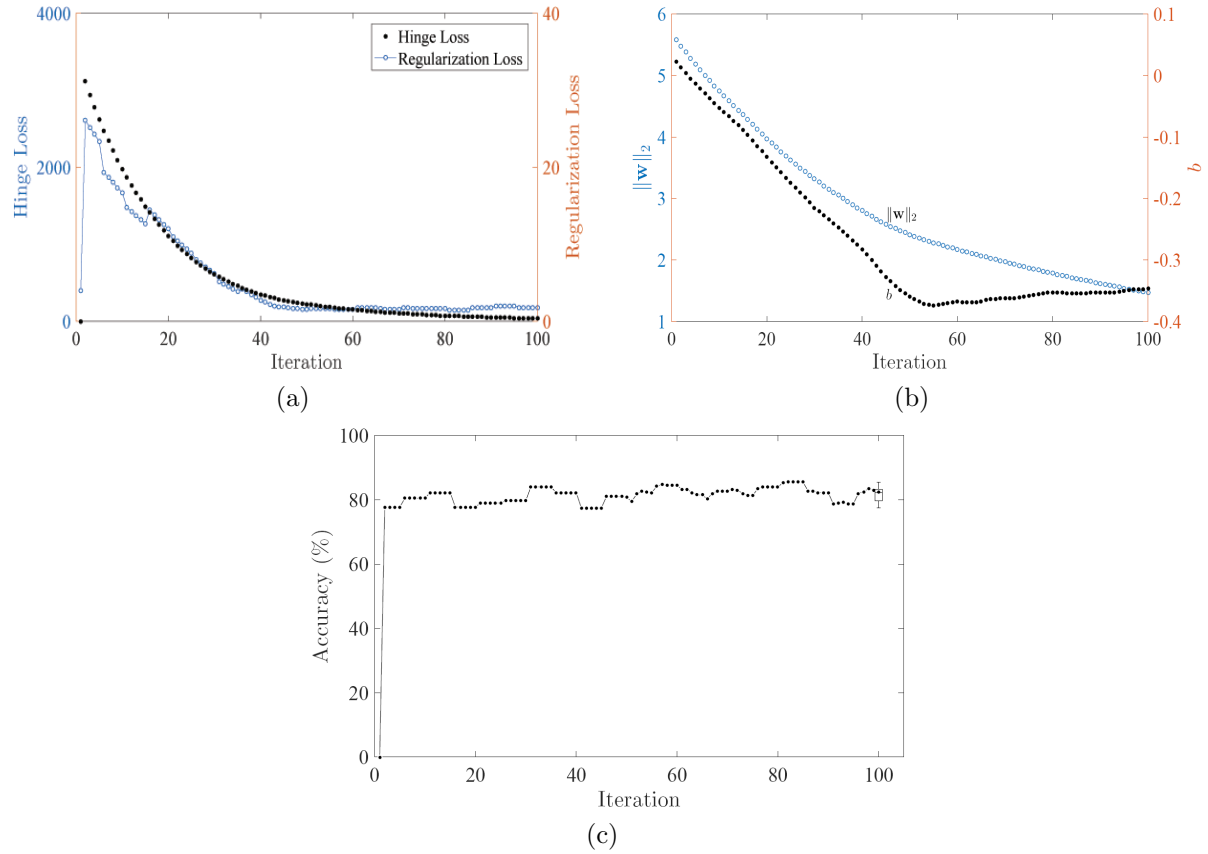

FIGURE 6. The evolution of loss functions (panel a), the model coefficients $\|\mathbf{w}\|_2$ and b (panel b), and the accuracy (panel c) during iteration

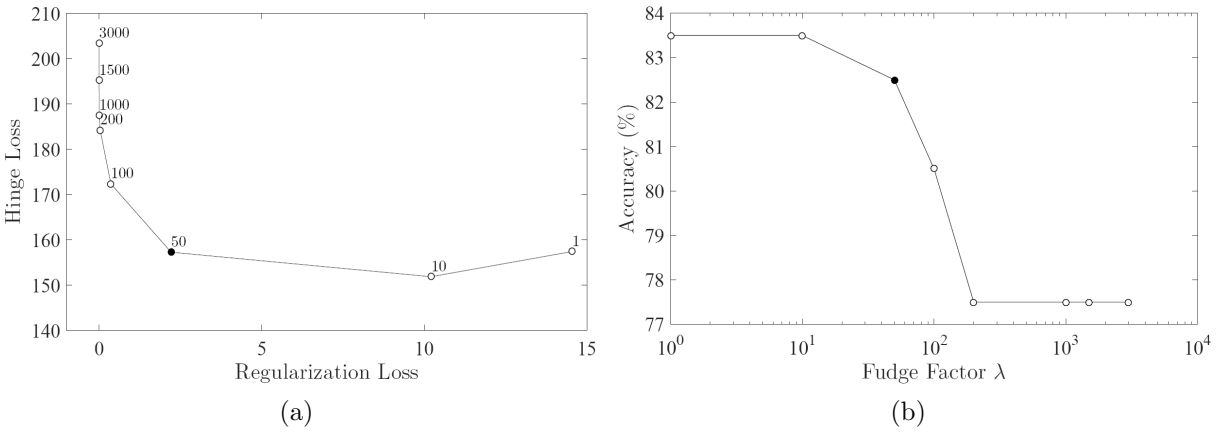

FIGURE 7. (a) The regularization loss versus the hinge loss. The best solution is obtained at $\lambda = 50$. (b) The effects of the fudge factor λ to the prediction accuracy during the training phase.

this factor is set to zero, the best model only satisfies the least-square criterion. The best fudge factor is obtained from an iterative process where the model coefficients are computed for various values of the fudge factor. The effects of the fudge factor to the two functions are shown in Figure 7. The hinge loss, measuring the fitness of the model to the data, tends to increase by increasing the fudge factor. A high value of the hinge loss denotes poor fitness. The values of the hinge loss are relatively similar for the fudge factor values of 1, 10, and 50. On the contrary, the regularization loss, measuring the level of over fitting, tends to decrease with increasing the factor. A high value of the

regularization loss denotes over fitting. The best fudge factor ($\lambda = 50$) is located on the bottom-left corner of the curve, providing a model that optimally fits the data.

The effects of the fudge factor to the model prediction accuracy during the training phase are depicted in Figure 7(b). If the fudge factor is set to a small value, the model may reach the accuracy of around 83.5%. However, this model over fits the data and may perform poorly for different batches of data. For the fudge factor of 50, which is the optimum value, the model accuracy is slightly lower at around 82.5%.

3.5. **The performance of the current approach.** The best model obtained at the fudge factor of 50 and trained at the rate of 1×10^{-4} is tested by using 500 batches of data. The results (Figure 8) show that the accuracy is in 76.8-87.5 percents. The accuracies of the two phases are relatively comparable indicating the model is generally applicable.

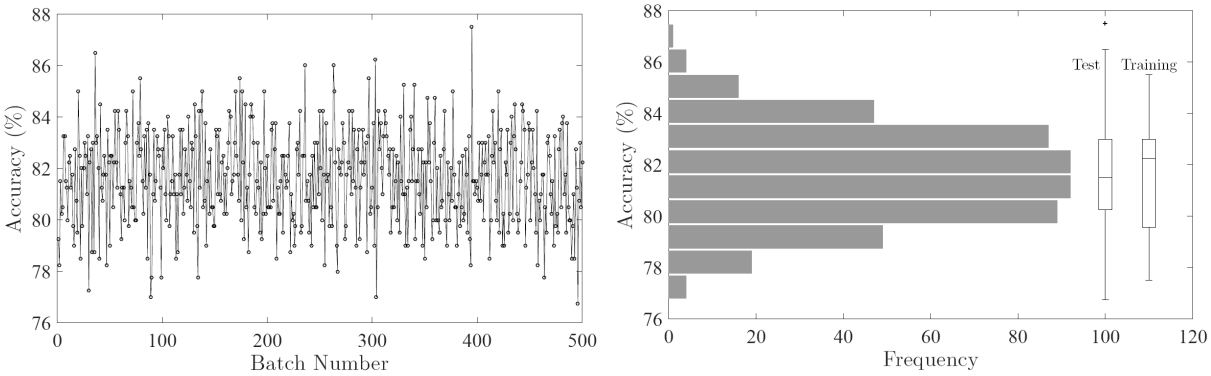

FIGURE 8. (a) The model accuracy during the testing phase; (b) the histogram and boxplot of the model accuracy during the testing phase

4. **Conclusions.** We present a solution to the problem associated with the use of F-statistic for SHM based on structural vibration data. The traditional method considers the structure to be damaged when the structure vibration data provide an estimate of F-statistic larger or smaller than the critical values or mathematically, and F-statistic satisfies any of the conditions: $F > F_{(\alpha/2,2K,2K)}$ or $F < F_{(1-\alpha/2,2K,2K)}$. The traditional classification method is demonstrated to be less reliable. For example, an analysis performed on the data obtained from a typical structural model shows that it can only achieve the level of accuracy of 72.6%. The method often labels the healthy structure as damaged leading to a false-positive signal. This work shows that the accuracy is improved when the classification method is revised to a simple linear model of $\mathbf{w}^T\mathbf{x}+b$ where $\mathbf{x}$ is a vector containing a few largest and smallest F-statistic values. This revision allows us to take account of several F-statistic values such that the classification accuracy can be increased by about 10% to the level of 81.5%.

During our investigation, we witness that the largest or smallest F-statistic value is a reliable damage indicator when the damage level is significant, but they are not reliable when the damage level is small. Moreover, we also witness that the variability of the F-statistic values seems increasing with the damage level. This fact is worthy for further investigation. In general, the future work should be addressed to find a damage-sensitive statistic representing F-statistic values. Some potential statistic descriptives are the maximum, minimum, range, standard deviation, and interquartile range.

REFERENCES

[1] Antara, *Collapsed Bridge Death Toll Rises to 19*, http://www.thejakartapost.com/news/2011/11/30/collapsed-bridge-death-toll-rises-to-19.html, 2011.

[2] BBC, *Brazil Flyover Collapses on Bus in Belo Horizonte*, http://www.bbc.com/news/world-latin-america-28154828, 2014.

[3] S. Gopalakhrishnan, M. Ruzzene and S. Hanagud, *Computational Techniques for Structural Health Monitoring*, Springer, 2011.

[4] S. Findlay and N. Harrison, Why aircraft fail, *Materials Today*, vol.5, no.11, pp.18-25, 2002.

[5] J. Schijve, Multiple-site damage in aircraft fuselage structures, *Fatigue & Fracture of Eng. Mat. & Struc.*, vol.18, pp.329-344, 1995.

[6] A. Widodo and B. S. Yang, Support vector machine in machine condition monitoring and fault diagnosis, *Mechanical Systems and Signal Processing*, vol.21, no.6, pp.2560-2574, 2007.

[7] R. B. Randall, *Vibration-Based Condition Monitoring: Industrial, Aerospace, and Automotive Applications*, John Wiley & Sons, 2011.

[8] J. R. Mohanty, B. B. Verma, D. R. K. Parhi and P. K. Ray, Application of artificial neural network for predicting fatigue crack propagation life of aluminum alloys, *Archives of Computational Materials Science and Surface Engineering*, vol.1, no.3, pp.133-138, 2009.

[9] M. M. Alamdari, T. Rakotoarivelo and N. L. D. Khoa, A spectral-based clustering for structural health monitoring of the Sydney harbor bridge, *Mech. Systems and Signal Processing*, vol.87, pp.384-400, 2017.

[10] P. Moser and B. Moaveni, Design and deployment of a continuous monitoring system for the downling hall footbridge, *Experimental Techniques*, vol.37, pp.15-26, 2013.

[11] A. Cigada, G. Moschioni, M. Vanali and A. Caprioli, The measurement network of the San Siro Meazza Stadium in Milan: Origin and implementation of a new data acquisition strategy for structural health monitoring, *Experimental Techniques*, vol.34, pp.70-81, 2010.

[12] D. Kang, D.-H. Kim and S. Jang, Design and development of structural health monitoring system for smart railroad-gauge-facility using FBG sensors, *Experimental Techniques*, vol.38, pp.39-47, 2014.

[13] P. Rolek, S. Bruni and M. Carboni, Condition monitoring of railway axles based on low frequency vibrations, *International Journal of Fatigue*, 2015.

[14] P. Nguyen, M. Kang, J.-M. Kim, B.-H. Ahn, J.-M. Ha and B.-K. Choi, Robust condition monitoring of rolling element bearings using de-noising and envelope analysis with signal decomposition techniques, *Expert Systems with Applications*, vol.42, no.22, pp.9024-9032, 2015.

[15] K. Jones and T. Athwal, Real-time patient weight monitoring system for chair based renal dialysis, *Journal of Biomedical Engineering*, vol.11, pp.300-302, 1989.

[16] C. Katsikeros and G. Labeas, Development and validation of a strain-based structural health monitoring system, *Mechanical Systems and Signal Processing*, vol.23, no.2, pp.372-383, 2009.

[17] A. Candelieri, R. Sormani, G. Arosio, I. Giordani and F. Archetti, Assessing structural health of helicopter fuselage panels through ANN hierarchies, *Int. J. of Reliability and Safety*, vol.7, pp.216-234, 2013.

[18] A. Candelieri, R. Sormani, G. Arosio, I. Giordani and F. Archetti, A hyper-solution SVM classification framework: Application to on-line aircraft structural health monitoring, *Procedia – Social and Behavioral Sciences*, vol.108, pp.57-68, 2014.

[19] M. S. Mhaske and R. S. Shelke, Detection of crack location and depth in a cantilever beam vibration measurement and its comparative validation in ANN and GA, *Int. J. of Res. in Eng. & Tech.*, vol.4, pp.152-157, 2015.

[20] F. Archetti, G. Arosio, A. Candelieri, I. Giordani and R. Sormani, Smart data driven maintenance: Improving damage detection and assessment on aerospace structures, *Metrology for Aerospace*, pp.101-106, 2014.

[21] W. Nick, J. Shelton, K. Asamene and E. Albert, A study of supervised machine learning techniques for structural health monitoring, *Proc. of the 26th Modern AI and Cognitive Science Conference*, Greensboro, NC, USA, vol.1353, pp.133-138, 2015.

[22] J. R. Mohanty, B. B. Verma, P. K. Ray and D. R. K. Parhi, Application of adaptive neuro-fuzzy inference system in modeling fatigue life under interspersed mixed-mode (I and II) spike overload, *Expert Systems with Applications*, vol.38, no.10, pp.12302-12311, 2011.

[23] J. R. Mohanty, B. B. Verma, P. K. Ray and D. R. K. Parhi, Prediction of mode-I overload-induced fatigue crack growth rates using neuro-fuzzy approach, *Expert Systems with Applications*, vol.37, no.4, pp.3075-3087, 2010.

[24] L. Yu, J. H. Zhu and L. L. Yu, Structural damage detection in a truss bridge model using fuzzy clustering and measured FRF data reduced by principal component projection, *Advances in Structural Engineering*, vol.16, no.1, pp.207-217, 2013.

[25] F. dos Santos, B. Peeters, H. V. der Auweraer, L. Goes and W. Desmet, Vibration-based damage detection for a composite helicopter main rotorblade, *Mech. Sys. & Signal Proc.*, vol.3, pp.22-27, 2016.

[26] R. de Medeiros, M. Sartorato, D. Vandepitte and V. Tita, A comparative assessment of different frequency based damage detection in unidirectional composite plates using MFC sensors, *J. of Sound and Vibration*, vol.383, pp.171-190, 2016.

[27] M. M. Quinones, L. A. Montejo and S. Jang, Experimental and numerical evaluation of wavelet based damage detection methodologies, *International Journal of Advanced Structural Engineering (IJASE)*, vol.7, no.69-80, 2015.

[28] N. G. Pnevmatikos and G. D. Hatzigeorgiou, Damage detection of framed structures subjected to earthquake excitation using discrete wavelet analysis, *Bulletin of Earthquake Engineering*, vol.15, no.1, pp.227-248, 2017.

[29] M. Pedram, A. Esfandiari and M. R. Khedmati, Damage detection by a FE model updating method using power spectral density: Numerical and experimental investigation, *J. of Sound and Vibration*, 2017.

[30] M. Cao, M. Radzieński, W. Xu and W. Ostachowicz, Identification of multiple damage in beams based on robust curvature mode shapes, *Mechanical Systems and Signal Processing*, vol.46, no.2, pp.468-480, 2014.

[31] E.-T. Lee and H.-C. Eun, Structural damage detection by power spectral density estimation using output-only measurement, *Shock and Vibration*, vol.2016, pp.2016-2022, 2016.

[32] D. D. Mandal, D. Wadadar and S. Banerjee, Performance evaluation of damage detection algorithms for identification of debond in stiffened metallic plates using a scanning laser vibrometer, *Journal of Vibration and Control*, 2017.

[33] U. Baneen and Z. Kausar, A baseline-free modal strain energy method for damage localisation, *Int. J. of Civil Eng.*, vol.10, pp.1-12, 2017.

[34] M. M. Alamdari, B. Samali, J. Li, H. Kalhori and S. Mustapha, Spectral-based damage identification in structures under ambient vibration, *J. Comput. Civ. Eng.*, vol.30, 2015.

[35] H. Sohn, J. A. Czarnecki and C. R. Farrar, Structural health monitoring using statistical process control, *Journal of Structural Engineering*, vol.126, no.11, pp.1356-1363, 2000.

[36] I. Mituletu, N. Gillich, C. Nitescu and C. Chioncel, A multi-resolution based method to precise identify the natural frequencies of beams with application in damage detection, *J. of Physics: Conf. Series*, vol.628, pp.12-20, 2015.

[37] G. Gillich, I. Mituletu, Z. Praisach, I. Negru and M. Tufoi, Method to enhance the frequency readability for detecting incipient structural damage, *Iranian Journal of Science and Technology, Transactions of Mechanical Engineering*, vol.41, no.3, pp.233-242, 2017.

[38] G.-R. Gillich and Z.-I. Praisach, Modal identification and damage detection in beam-like structures using the power spectrum and time-frequency analysis, *Signal Processing*, vol.96, pp.29-44, 2014.

[39] G. Gillich, I. Mituletu, I. Negru, M. Tufoi, V. Iancu and F. Muntean, A method to enhance frequency readability for early damage detection, *J. of Vibration Eng. Tech.*, vol.3, pp.637-652, 2015.

[40] S. D. Fassois and J. S. Sakellariou, Chapter 23: Statistical time series methods for SHM, in *Encyclopedia of Structural Health Monitoring*, John Wiley & Sons, 2009.

[41] F. Kopsaftopoulos and S. Fassois, Vibration based health monitoring for a lightweight truss structure: Experimental assessment of several statistical time series methods, *Mechanical Systems and Signal Processing*, vol.24, no.7, pp.1977-1997, 2010.

[42] C. R. Farrar and K. Worden, *Structural Health Monitoring: A Machine Learning Perspective*, John Wiley & Sons, 2012.

[43] R. J. Schilling and S. L. Harris, *Fundamentals of Digital Signal Processing Using MATLAB*, Cengage Learning, 2011.

[44] F. E. Gunawan, Impact force reconstruction using the regularized Wiener filter method, *Inverse Problems in Science and Engineering*, vol.24, no.7, pp.1107-1132, 2016.

[45] N. Christianni and J. Shawe-Taylor, *An Introduction to Support Vector Machines and Other Kernel-Based Learning Methods*, Cambridge University Press, 2000.

[46] T. Hastie, R. Tibshirani and J. Friedman, *The Elements of Statistical Learning*, Springer, 2008.

[47] D. M. W. Powers, *Evaluation: From Precision, Recall and F-measure to ROC, Informedness, Markedness & Correlation*, TR-SIE-07-001, Flinders Univ., Australia, 2007.